

The (g-2) intermediate window quantity from a coordinate-space method

En-Hung Chao^{a,d} **Harvey B. Meyer**^{a,b,c} and **Julian Parrino**^{a,*}

^a*PRISMA+ Cluster of Excellence & Institut für Kernphysik,
Johannes Gutenberg-Universität Mainz, D-55099 Mainz, Germany*

^b*Helmholtz Institut Mainz,
Staudingerweg 18, D-55128 Mainz, Germany*

^c*GSI Helmholtzzentrum für Schwerionenforschung,
D-64291 Darmstadt, Germany*

^d*Physics Department, Columbia University, New York, New York 10027, USA*

E-mail: juparrin@uni-mainz.de

We present a calculation of the intermediate window quantity of the hadronic vacuum polarization contribution to the muon g-2 using a Lorentz-covariant coordinate-space method at a fixed pion mass of 350 MeV. This method is more flexible in the choice of the integration kernel than the time-momentum representation and gives a different perspective on the systematic errors of the g-2 calculation. It furthermore serves as a check for the recent results of the Mainz group.

*The 39th International Symposium on Lattice Field Theory,
8-13 August 2022,
Bonn, Germany*

*Speaker

1. Introduction

The anomalous magnetic moment of the muon is a well suited quantity for precision tests of the standard model. With the published results of the E989 Experiment at Fermilab in 2021 confirming the earlier measurement at BNL the experimental world average is under a 4.2σ tension with the white paper result from the theory side in 2020, see Ref. [1]. However, there is also a full lattice calculation claiming a smaller deviation from the experimental result, see Ref. [2]. It is therefore of high interest to further investigate the theory calculation of this quantity. The largest part of the standard model result comes from pure QED effects. But, the main part of the uncertainty is due to hadronic effects. These effects need to be addressed non-perturbatively because of the running coupling of QCD. They can be classified through the order of the electromagnetic coupling α_{QED} they are multiplying. The leading hadronic contribution to $O(\alpha_{\text{QED}}^2)$ is the hadronic vacuum polarization. There are two approaches to calculate this quantity: the data-driven approach and the determination with lattice QCD. Recently a tension between the two approaches is observed. A proposal for understanding the tension is to compare the intermediate window observable a_μ^{W} , first introduced in Ref. [3] computed in both approaches. This observable is less sensitive to lattice artifacts, so it can be calculated with sub-percent precision. Many collaborations have recently come up with results for this quantity. On the side of the data-driven approach the window observable is expressed by modifying the relevant kernel function. The latest results on this are given in Ref. [4].

So far, all lattice results for a_μ^{W} are calculated using the time-momentum representation (TMR) [5], which involves a Euclidean-time correlation function calculated at vanishing spatial momentum. Here, we focus on a different formulation using a covariant coordinate space (CCS) framework, first proposed in Ref. [6]. As there is a family of possible CCS kernel functions, this method offers a more flexible way of implementing the spatial integral. Another motivation for choosing this method is that in this framework lattice artifacts can be very different. In that sense, the CCS method gives a different point of view on the continuum extrapolation of the lattice data and therefore a valid check for the results obtained in the TMR method.

We present results for the isovector and strange-connected contribution to the window quantity in the CCS method at an unphysical pion mass of ~ 350 MeV with 4 different lattice spacings. The complete details of the calculation can be found in Ref. [7], where the results for the two considered channels are extrapolated to the reference point $(m_\pi, m_K) = (350 \text{ MeV}, 450 \text{ MeV})$. The aim of this proceeding is as follows: We outline the important parts of the calculation, with just the necessary information to understand the procedure. We refer the reader to Ref. [7] for technical details. We recall the window quantity in the TMR formulation in Sect. 2 and discuss its associated CCS representation in Sect. 3. We give details on the chosen lattice setup in Sect. 4. In Sect. 5 the model for correcting for finite-size effects is explained. In Sect. 6, a preliminary study of the chiral and continuum extrapolation is performed, where the pion-mass dependence in the continuum limit is assumed to be identical to that of the TMR-based Mainz 2022 result, Ref. [8].

2. Time-momentum representation

The state-of-the-art method to calculate the hadronic vacuum polarization contribution to the anomalous magnetic moment of the muon a_μ^{hvp} on the lattice is based on the time-momentum

representation (TMR) (see [5])

$$a_{\mu}^{\text{hvp}} = \left(\frac{\alpha}{\pi}\right)^2 \int_0^{\infty} dt f(t, m_{\mu}) G(t) \quad (1)$$

where $G(t)$ is the spatially-summed two-point correlator

$$G(t) = -\frac{1}{3} \sum_{i=1}^3 \int d^3x \langle j_i(x) j_i(0) \rangle \quad (2)$$

and $f(t, m_{\mu})$ is the TMR kernel function, with $\hat{t} = tm_{\mu}$

$$f(t, m_{\mu}) = \frac{2\pi^2}{m_{\mu}^2} \left(-2 + 8\gamma_E + \frac{4}{\hat{t}^2} + \hat{t}^2 - \frac{8K_1(2\hat{t})}{\hat{t}} + 8 \ln(\hat{t}) + G_{1,3}^{2,1} \left(\hat{t}^2 \middle| \begin{matrix} \frac{3}{2} \\ 0, 1, \frac{1}{2} \end{matrix} \right) \right) \quad (3)$$

where K_1 is a modified Bessel function of the second kind and $G_{p,q}^{m,n}$ is a Meijer function. As first presented in Ref. [3] it is possible to restrict the integration region of Eq. (1) to an intermediate window by using a smooth heaviside function $\theta_{\Delta}(t) = \frac{1}{2}(1 + \tanh(\frac{t}{\Delta}))$. The kernel function is then transformed in the following way

$$f_W(t, m_{\mu}) = \left(\frac{\alpha}{\pi}\right)^2 (\theta_{\Delta}(t - t_0) - \theta_{\Delta}(t - t_1)) \cdot f(t, m_{\mu}) \quad (4)$$

where the values for the standard intermediate window are $t_0 = 0.4$ fm, $t_1 = 1.0$ fm and $\Delta = 0.15$ fm. The window quantity in the TMR formulation then reads

$$a_{\mu}^{\text{W}} = \int_0^{\infty} dt f_W(t, m_{\mu}) G(t) \quad (5)$$

It is analogously possible to define a short-distance window quantity a_{μ}^{SD} by using $t_0^{\text{SD}} = 0$ fm, $t_1^{\text{SD}} = 0.4$ fm and a long-distance window quantity a_{μ}^{LD} with $t_0^{\text{LD}} = 1.0$ fm, $t_1^{\text{LD}} = \infty$, where $\Delta = 0.15$ fm is fixed. The total hadronic contribution a_{μ}^{hvp} is then easily recovered through

$$a_{\mu}^{\text{hvp}} = a_{\mu}^{\text{SD}} + a_{\mu}^{\text{W}} + a_{\mu}^{\text{LD}}. \quad (6)$$

This allows for a different treatment of each of the individual contributions using different methods. The intermediate window quantity is well suited for lattice calculations, because it is less sensitive to lattice artifacts. This comes from the fact that the short-distance region, where cut-off effects are expected to be significant as well as the long-distance region, where finite-size effects are a dominant source of error, are highly suppressed in the calculation of this observable.

3. Covariant coordinate-space method

A different approach for the calculation of a_{μ}^{W} is the covariant coordinate-space (CCS) method introduced in Ref. [6]. As worked out in Ref. [7] the intermediate window quantity defined in Eq. (5) can be translated into a CCS formulation as well:

$$a_{\mu}^{\text{W}} = \int d^4x H_{\mu\nu}(x) G_{\mu\nu}(x), \quad (7)$$

Id	β	$L^3 \times T$	a [fm]	m_π [MeV]	m_K [MeV]	$m_\pi L$	L [fm]	#confs light/strange
U102	3.4	$24^3 \times 96$	0.08636	353(4)	438(4)	3.7	2.1	200/0
H102		$32^3 \times 96$				4.9	2.8	240/120
S400	3.46	$32^3 \times 128$	0.07634	350(4)	440(4)	4.2	2.4	240/120
N203	3.55	$48^3 \times 128$	0.06426	346(4)	442(5)	5.4	3.1	$90 \times 2/90 \times 2$
N302	3.7	$48^3 \times 128$	0.04981	346(4)	450(5)	4.2	2.4	240/120

Table 1: Overview of the used ensembles. The lattice spacings are determined in Ref. [9] and the pion and kaon masses are taken from Ref. [8].

where $G_{\mu\nu}(x) = \langle j_\mu(x)j_\nu(0) \rangle$ is the vector-vector correlator and the CCS Kernel function can be determined by:

$$H_{\mu\nu}(x) = -\delta_{\mu\nu}\mathcal{H}_1(|x|) + \frac{x_\mu x_\nu}{|x|^2}\mathcal{H}_2(|x|) \quad (8)$$

with

$$\mathcal{H}_1(|x|) = \frac{2}{9\pi|x|^4} \int_0^{|x|} dt \sqrt{|x|^2 - t^2} (2|x|^2 + t^2) f_W(t, m_\mu) \quad (9)$$

$$\mathcal{H}_2(|x|) = \frac{2}{9\pi|x|^4} \int_0^{|x|} dt \sqrt{|x|^2 - t^2} (4t^2 - |x|^2) f_W(t, m_\mu). \quad (10)$$

Using the fact that the continuum vector-vector correlator is conserved $\partial_\mu G_{\mu\nu} = 0$, it is possible to add a term to the CCS Kernel function $\tilde{H}_{\mu\nu}(x) = H_{\mu\nu}(x) + \partial_\mu(x_\nu g(|x|))$ which amounts only to a surface term that vanishes in infinite volume. This means that there is a family of kernel functions $\tilde{H}_{\mu\nu}(x)$ resulting in the same integral, but with a differently-shaped integrand. This is an advantage in contrast to the TMR method, where the kernel function $f(t, m_\mu)$ is fixed. When choosing an appropriate kernel function, there are two main considerations one has to take into account. A short-ranged kernel function is often preferred in order to suppress the noisy behaviour of the tail of the integrand. Another criterion is the control over finite-size effects. It is desirable to choose a kernel function that results in small finite-size effects. As explained in Ref. [7], for the ensembles we use, the finite-size effects were best controlled using the traceless kernel function

$$H_{\mu\nu}^{\text{TL}}(x) = \left(-\delta_{\mu\nu} + 4 \frac{x_\mu x_\nu}{|x|^2} \right) \mathcal{H}_2(|x|). \quad (11)$$

4. Lattice setup

We use five different $N_f = 2 + 1$ flavor gauge ensembles generated by the Coordinated Lattice Simulations consortium [10] with a pion mass around 350 MeV. These ensembles have been generated with the $O(a)$ -improved Wilson-Clover fermion action and tree-level $O(a^2)$ improved Lüscher-Weisz gauge action. Details about the used ensembles can be found in Tab. 1. The lattice spacings were determined in Ref. [9] and the pion and kaon masses are taken from Ref. [8]. Open

boundary conditions are employed for all of the listed ensembles. For the ensemble N203, two replica have been included in the analysis. We calculate only the highly dominant isovector and the strange-connected contribution. In order to control discretization effects, we use two different formulations of the vector current, the local (L)

$$j_\mu^{(L)}(x) = \bar{\psi}(x)\gamma_\mu\mathcal{Q}\psi(x), \quad (12)$$

and conserved (C)

$$j_\mu^{(C)}(x) = \frac{1}{2} \left(j_\mu^{(N)}(x) + j_\mu^{(N)}(x - a\hat{\mu}) \right), \quad (13)$$

$$j_\mu^{(N)}(x) = \frac{1}{2} \left[\bar{\psi}(x + a\hat{\mu})(1 + \gamma_\mu)U_\mu^\dagger(x)\mathcal{Q}\psi(x) - \bar{\psi}(x)(1 - \gamma_\mu)U_\mu(x)\mathcal{Q}\psi(x + a\hat{\mu}) \right], \quad (14)$$

where $U_\mu(x)$ is the gauge link and \mathcal{Q} is a generic quark charge matrix acting in flavor space. We furthermore use the improved vector current

$$j_\mu^{(\alpha),I}(x) = j_\mu(x) + ac_V^{(\alpha)}\partial_\nu T_{\mu\nu}(x), \quad \text{for } \alpha = L, C, \quad (15)$$

where the local tensor current is defined by $T_{\mu\nu} \equiv -\frac{1}{2}\bar{\psi}(x)[\gamma_\mu, \gamma_\nu]\mathcal{Q}\psi(x)$ and $c_V^{(\alpha)}$ is an improvement coefficient. The conserved current $j_\mu^{(C)}(x)$ does not need to be renormalized. However, the local current does need a multiplicative renormalization factor

$$j_\mu^{(L),R}(x) = \hat{Z}_V^{(L)} j_\mu^{(L),I}(x). \quad (16)$$

where we use the values for the factor $\hat{Z}_f^{(L)}$ and the coefficient $c_V^{(\alpha)}$ determined non-perturbatively in Ref. [11].

To calculate a_μ^W using Eq. (7), we do not need to store the full position space correlator $\langle j_i(x)j_i(0) \rangle$. But, using the fact that the CCS kernel function in Eq. (8) is split into two Lorentz scalars, one multiplying $x_\mu x_\nu$ and the other multiplying $\delta_{\mu\nu}$, we only need to calculate the functions

$$\widehat{G}_1^{\text{conn.}}(r) = -\text{Tr}\{\mathcal{Q}^2\} \sum_{x \in \Lambda, |x|=r} \Re \text{Tr}[S(x,0)\gamma_\mu S(0,x)\gamma_\mu], \quad (17)$$

$$\widehat{G}_2^{\text{conn.}}(r) = -\text{Tr}\{\mathcal{Q}^2\} \sum_{x \in \Lambda, |x|=r} \Re \text{Tr}[S(x,0)\not{x}S(0,x)\not{x}], \quad (18)$$

where $S(x,0)$ is the quark propagator for the light or the strange contribution. For the $O(a)$ improvement term it is necessary to calculate a third function

$$\widehat{G}_3^{\text{conn.}}(r) = -\text{Tr}\{\mathcal{Q}^2\} \sum_{x \in \Lambda, |x|=r} \Re \text{Tr}[S(x,0)\gamma_\mu S(0,x)(\not{x}\gamma_\mu - \gamma_\mu\not{x})]. \quad (19)$$

This fact was previously discussed in Ref. [12]. Eqs. (17 - 19) hold for the case of two local vector currents (LL). Additionally, we calculate the functions $G_i^{\text{conn.}}$ for the case, where one of the currents is conserved. Deriving analogous expressions for the conserved-local (CL) case is straightforward.

Id	CCS method $H_{\mu\nu}^{\text{TL}}$ kernel				TMR method			
	isovector		strange		isovector		strange	
	(LL)	(CL)	(LL)	(CL)	(LL)	(CL)	(LL)	(CL)
U102	174.26(191)	164.78(190)	—	—	—	—	—	—
H102	177.83(92)	168.66(90)	35.66(19)	33.54(19)	178.54(52)	179.75(52)	35.66(12)	35.90(11)
S400	175.21(96)	167.57(94)	34.90(20)	33.15(20)	173.82(69)	174.49(68)	34.402(86)	34.548(82)
N203	173.25(89)	167.60(88)	34.11(14)	32.83(13)	173.75(43)	174.11(43)	34.225(90)	34.283(89)
N302	169.08(96)	165.39(95)	33.31(17)	32.46(17)	167.77(87)	167.84(87)	32.427(83)	32.444(82)

Table 2: Comparison between the results for the light connected and strange contribution obtained in the CCS method using spherical integration and the results of the Mainz group [8] using the TMR method. Finite size corrections are applied to the light connected contribution for both methods. The results for U102 are not included in the final analysis, due to the reasons explained in Ref. [7]. All values are in units of 10^{-10} .

5. Correction for the finite-size effects

At the aimed level of precision it is necessary to correct the data in the isovector channel for finite-size effects (FSE). The largest contribution to this correction comes from two-pion intermediate states. In the literature, many approaches have been developed for the TMR method, see Ref. [1] for further references. For our position-space calculation, it is most convenient and transparent to start with field theoretic approach. We decided to base our FSE corrections on the model described in Ref. [13], with the Lagrangian in Euclidean spacetime

$$\begin{aligned} \mathcal{L} = & \frac{1}{4}F_{\mu\nu}(A)^2 + \frac{1}{4}F_{\mu\nu}(\rho)^2 + \frac{1}{2}m_\rho^2\rho_\mu^2 + \frac{e}{2g_\gamma}F_{\mu\nu}(A)F_{\mu\nu}(\rho) \\ & +(D_\mu\pi)^\dagger(D_\mu\pi) + m_\pi^2\pi^\dagger\pi \end{aligned} \quad (20)$$

with the covariant derivative $D_\mu \equiv \partial_\mu - ieA_\mu - ig\rho_\mu$. The degrees of freedom of this theory are described by the pion π , the photon A_μ and the massive rho meson ρ_μ . We will refer to this as the Sakurai QFT. As explained in Ref. [13] this theory is able to reproduce the Gounaris-Sakurai parametrization of the pion electric formfactor. Starting from a Lagrangian formulation, it is straightforward to renormalize the theory in infinite volume. The current-current correlator computed in lattice QCD corresponds to $\frac{\delta^2 \log Z[A]}{\partial A_\mu(x)\partial A_\nu(y)}$, where $Z[A]$ is the partition function. This is calculated in the Sakurai QFT in finite and infinite volume. The difference of this is added as a finite-size correction to the result for a_μ^{W} calculated on each ensemble. For this calculation we use the specific parameters for the pion and rho mass on each ensemble given in Ref. [14]. We do not correct the strange-connected contribution for finite-size effects.

6. Continuum extrapolation

The results for each individual ensemble calculated in the CCS representation are displayed in Tab. 2 together with the recent results of the Mainz group using the TMR representation [8]. The results for the isovector contribution for both methods are corrected for finite-size effects. We observe that the results for the (LL) discretization for the larger ensembles H102 and N203 are in good agreement with the results for the TMR method, while the results for S400 and N302 are slightly higher. On the other hand the results for the (CL) discretization are very different. These are much lower, than in the TMR method, especially for the coarser lattice spacings. This is not a

contradiction since only the continuum results have to agree and both methods can have different $O(a^2)$ effects. The data furthermore suggests that the continuum extrapolation for the (CL) data in the CCS method is expected to be flatter than for the TMR method. This is illustrated in Fig. 1.

At this point, we want to account for the differences in the pion and kaon masses of the chosen ensembles, given in Tab. 1. It is possible to shift each of the results to the same reference point in the (m_π, m_K) -plane by using the global fit from the TMR method evaluated in Ref. [8]. This shift is done ensemble-by-ensemble at the corresponding lattice spacings. Since both methods have different discretization errors, this introduces an additional systematic error. In Ref. [7] the reference point $(m_\pi, m_K) = (350 \text{ MeV}, 450 \text{ MeV})$ is chosen very close to the corresponding pion and kaon masses of the used ensembles. This means that the shifts added to the individual ensembles are very small and the systematic error for this procedure is almost negligible.

Since we have fully implemented the Symanzik improvement scheme, the $O(a)$ effects are absent in the continuum extrapolation and we can safely perform a fit linear in a^2

$$f_1(a, \alpha_1, \beta_1) = \alpha_1 + \beta_1 a^2. \quad (21)$$

To get an estimate on the systematic error of this fitting procedure we also perform fits involving a^3 , $a^2 \log(a)$ and $a^2/\log(a)$ terms and cuts in the lattice spacing. The systematic error is then obtained by calculating the root-mean-square deviation from the individual fit results from their average. For our final result, we evaluate the plain average between the (CL) and (LL) discretization with the statistical error coming from the error of the fit. As the final results for the isovector and strange-connected channel of the hadronic vacuum polarization contribution to the anomalous magnetic moment of the muon at the reference point $(m_\pi, m_K) = (350 \text{ MeV}, 450 \text{ MeV})$, we quote the results from Ref. [7]

$$\left(a_\mu^{\text{W,I1}}\right)_{\text{ref}} = 165.17(157)_{\text{stat}}(99)_{\text{syst}} \times 10^{-10}, \quad (22)$$

$$\left(a_\mu^{\text{W,s}}\right)_{\text{ref}} = 32.49(22)_{\text{stat}}(23)_{\text{syst}} \times 10^{-10}. \quad (23)$$

For a complete evaluation of a_μ^{W} at the physical point, a more thorough analysis on the chiral extrapolation becomes necessary. Eventually, one has to include ensembles with light pion-masses to determine the meson-mass dependence in the CCS method, which could be different from the TMR at non-vanishing lattice spacings. But as an exploratory study, we assume the same meson-mass dependence as found for the TMR to calculate the necessary shift to $(m_\pi, m_K) = (134.9768 \text{ MeV}, 495.011 \text{ MeV})$ on an ensemble-by-ensemble basis. These shifts are displayed in Tab. 3. In Fig. 1 we show the continuum extrapolation at the physical point using Eq. (21) as the fit function. For this exploratory study, we quote 25% of the shift as systematic error for the procedure. The latter should be seen, however, as a naive estimate for the error. Using this method we obtain the following results for the isovector and the strange-connected contribution at the physical point

$$\left(a_\mu^{\text{W,I1}}\right)_{\text{phys}} = 186.38(175)_{\text{stat}}(90)_{\text{syst}}(x)_{\text{TMR}} \times 10^{-10}, \quad (24)$$

$$\left(a_\mu^{\text{W,s}}\right)_{\text{phys}} = 27.71(25)_{\text{stat}}(22)_{\text{syst}}(x)_{\text{TMR}} \times 10^{-10}. \quad (25)$$

The $(x)_{\text{TMR}}$ indicates that there is an additional systematic error associated with the fact that we assume the same chiral dependence as in the TMR method. However, the shifts calculated in

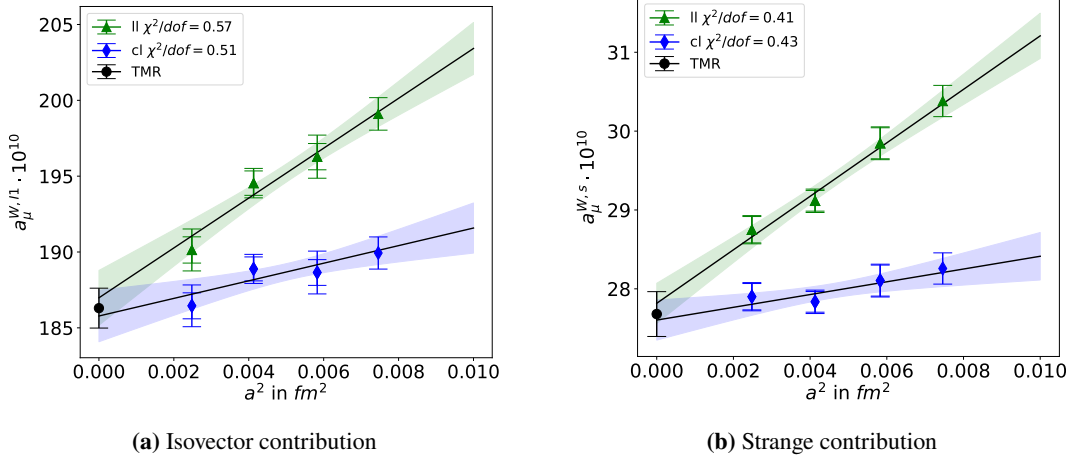


Figure 1: Continuum extrapolation at the reference point $m_\pi = 134.9768$ MeV and $m_K = 495.011$ MeV using the TL-kernel. The isovector contribution is corrected for finite-size effects. For the strange contribution no finite-size correction is applied. The smaller error bar is only the statistical error, the larger is the total error.

Tab. 3 are independent of the lattice spacing, due to the explicit form of the fit function from the TMR method. This suggests that this uncertainty is small. There is an additional uncertainty that we express by $(x)_{\text{TMR}}$, which comes from using only one fit from the TMR method. We do not account for the systematic uncertainty of this particular fit. A naive guess for the magnitude of this uncertainty is the total systematic error of the result in the TMR method, which is of the same order of magnitude as the systematic error of fitting procedure in the CCS method described above.

Id	isovector		strange	
	(LL)	(CL)	(LL)	(CL)
H102	21.51(54)	21.46(54)	-5.28(7)	-5.27(7)
S400	21.33(55)	21.28(55)	-5.05(7)	-5.04(7)
N203	20.66(53)	20.62(54)	-4.99(7)	-4.98(7)
N302	20.77(56)	20.71(56)	-4.56(6)	-4.56(6)

Table 3: Corrections to the physical point $m_\pi = 134.9768$ MeV $m_K = 495.011$ MeV calculated in the TMR method. All values are in units of 10^{-10}

7. Conclusion

After showing preliminary results at the lattice conference 2022, we have finalized the calculation of a_μ^W at an unphysical pion mass of $m_\pi = 350$ MeV. This provides a significant check for the calculation using the TMR method, where we refer to the results of the Mainz group [8]. In Ref. [7] the complete details of the calculation in the CCS method are shown, confirming the results of the TMR method. We have furthermore demonstrated in this proceeding that with the global fit using the results from the TMR method, it is possible to perform a naive extrapolation to the physical pion

and kaon mass, at the cost of additional systematic uncertainties. At first glance, the center values of these contributing channels are in good agreement with the published lattice results, although a more careful study of the chiral extrapolation and its associated error is still needed.

We have outlined the important steps of the calculation of a_μ^W in the CCS method, including the treatment of finite-size effects. This can be used as a guideline for the calculation of other interesting quantities on the lattice such as the hadronic contribution to the running of the QED coupling $\Delta\alpha$ or even other Euclidean time window quantities for the hadronic contribution to a_μ . The flexibility to choose a kernel function in the CCS methods offers a possibility to optimize the kernel function for a specific window. For a calculation of the short-distance window quantity it may be beneficial to choose a more long-ranged kernel, in order to suppress cut-off effects of the lattice.

Finally, we want to mention the application of the CCS representation for master-field simulations [15], where only a small amount of gauge configurations are simulated on a very large lattice. Since for these calculations, the necessary statistics is gathered from many different coordinate-space subvolumes of the master-field, a coordinate-space framework is well suited in order to perform the calculation of an observable. Therefore, the CCS representation might be favorable in this case.

References

- [1] T. Aoyama *et al.*, *Phys. Rept.* **887**, 1 (2020), arXiv:2006.04822 [hep-ph] .
- [2] S. Borsanyi *et al.*, *Nature* **593**, 51 (2021), arXiv:2002.12347 [hep-lat] .
- [3] T. Blum, P. A. Boyle, V. Gülpers, T. Izubuchi, L. Jin, C. Jung, A. Jüttner, C. Lehner, A. Portelli, and J. T. Tsang (RBC, UKQCD), *Phys. Rev. Lett.* **121**, 022003 (2018), arXiv:1801.07224 [hep-lat] .
- [4] G. Colangelo, A. X. El-Khadra, M. Hoferichter, A. Keshavarzi, C. Lehner, P. Stoffer, and T. Teubner, *Phys. Lett. B* **833**, 137313 (2022), arXiv:2205.12963 [hep-ph] .
- [5] D. Bernecker and H. B. Meyer, *Eur.Phys.J.* **A47**, 148 (2011), arXiv:1107.4388 [hep-lat] .
- [6] H. B. Meyer, *Eur. Phys. J. C* **77**, 616 (2017), arXiv:1706.01139 [hep-lat] .
- [7] E.-H. Chao, H. B. Meyer, and J. Parrino, (2022), arXiv:2211.15581 [hep-lat] .
- [8] M. Cè *et al.*, (2022), arXiv:2206.06582 [hep-lat] .
- [9] M. Bruno, T. Korzec, and S. Schaefer, *Phys. Rev. D* **95**, 074504 (2017), arXiv:1608.08900 [hep-lat] .
- [10] M. Bruno *et al.*, *JHEP* **02**, 043 (2015), arXiv:1411.3982 [hep-lat] .
- [11] A. Gerardin, T. Harris, and H. B. Meyer, *Phys. Rev. D* **99**, 014519 (2019), arXiv:1811.08209 [hep-lat] .

- [12] M. Cè, A. Gérardin, K. Ottnad, and H. B. Meyer, *PoS LATTICE2018*, 137 (2018), [arXiv:1811.08669 \[hep-lat\]](#) .
- [13] F. Jegerlehner and R. Szafron, *Eur. Phys. J. C* **71**, 1632 (2011), [arXiv:1101.2872 \[hep-ph\]](#) .
- [14] A. Gérardin, M. Cè, G. von Hippel, B. Hörz, H. B. Meyer, D. Mohler, K. Ottnad, J. Wilhelm, and H. Wittig, *Phys. Rev. D***100**, 014510 (2019), [arXiv:1904.03120 \[hep-lat\]](#) .
- [15] P. Fritsch, J. Bulava, M. Cè, A. Francis, M. Lüscher, and A. Rago, *PoS LATTICE2021*, 465 (2022), [arXiv:2111.11544 \[hep-lat\]](#) .